JOURNAL OF CATALYSIS **165,** 172–183 (1997)
ARTICLE NO. CA971487

Platinum-Promoted and Unpromoted Sulfated Zirconia Catalysts Prepared by a One-Step Aerogel Procedure

1. Physico-chemical and Morphological Characterization

C. Morterra,*[,1] G. Cerrato,* S. Di Ciero,* M. Signoretto,† F. Pinna,† and G. Strukul†

*Dipartimento di Chimica Inorganica, Chimica Fisica e Chimica dei Materiali, Università di Torino, Via Pietro Giuria 7, 10125 Torino, Italy; and †Dipartimento di Chimica, Università di Venezia, Calle Larga S. Marta 2137, 30123 Venezia, Italy

Received March 18, 1996; revised July 29, 1996; accepted September 30, 1996

Through a one-step sol-gel synthetic method, several sulfated zirconia systems with different sulfate content and several Pt-promoted sulfated zirconia systems with a fixed amount of sulfate and different amounts of Pt were prepared. S and Pt in the resulting catalysts were determined by analytical methods. Crystallographic and morphological features of the ZrO_2 support and, where present, of the supported Pt were examined by XRD and TEM. The adsorptive capacity of Pt-promoted systems toward H_2 and O_2 was determined with a pulse-flow system, and toward CO both with a pulse-flow system and by FTIR spectroscopy. FTIR was also used to characterize the sulfate species present at the surface of the various systems, and to evaluate the resistance of surface sulfates toward vacuum thermal treatments and toward reductive treatments at various temperatures; the latter property was also determined by TPR–MS. The preparation method leads to catalysts that are either pure tetragonal or mainly monoclinic, depending on the amount of sulfuric acid. Reductive treatments deactivate (shield) the exposed Pt, whereas oxidative treatments reactivate it; the presence of Pt, which is known to improve the performance and the stability of sulfated ZrO_2 systems, renders surface sulfates much easier to eliminate either by thermal treatment *in vacuo* or by reduction in H_2. © 1997 Academic Press

1. INTRODUCTION

Pt-promoted and unpromoted sulfated zirconia materials have recently emerged as the most promising contribution in the achievement of a new generation of catalysts for the isomerization of alkanes (1–8). These materials possess strong acid characteristics and are particularly suited for carrying out the above reaction under thermodynamically favorable conditions. This field of research has been extensively studied over the past few years and has witnessed an impressive growth of applications, although the role of platinum, the deactivation pathways, and the overall mechanism of action of these catalysts are still largely unknown.

The synthetic methods used to obtain this family of catalysts are numerous, although they are generally stepwise and involve similar operations. These synthetic differences produce catalysts that are only nominally similar, but possess different characteristics and are often difficult to compare. The problems involved in the different synthetic routes to promoted and unpromoted sulfated zirconia catalysts have recently been reviewed (9) and we have proposed (9) a reliable single stage sol-gel procedure as a potential method for overcoming some of the problems. A preliminary account of the present work, describing the synthetic details of the sol-gel method to produce aerogel materials, has been reported elsewhere (10). In this paper we report in some detail the physicochemical and morphological properties of these catalysts, whereas their activity in the isomerization of *n*-butane under a variety of conditions will be described in a later paper (Part 2).

2. EXPERIMENTAL

2.1. Catalyst Preparation

Pt-promoted (PZS) and unpromoted (AZS) sulfated zirconia materials have been prepared following the one-step procedure which has been described in detail elsewhere (10).

To prepare PZS samples, the proper amounts of *i*-PrOH, H_2SO_4 (96%), and $H_2PtCl_6 \cdot 6H_2O$ dissolved in *i*-PrOH (20 ml) and a 70% $Zr(OPr)_4$ solution in *i*-PrOH were placed in a conical flask. To this solution, a mixture of *i*-PrOH (60 ml) and H_2O (8.4 ml) was slowly added dropwise with stirring. When the addition was complete, the resulting mixture was stirred vigorously for 15 min and then left aside overnight at room temperature. When preparing the AZS samples, the addition of H_2PtCl_6 solution was obviously omitted.

[1] To whom correspondence should be addressed. Fax: +39.11.670 7855. E-mail: morterra@ch.unito. it.

0021-9517/97 $25.00
Copyright © 1997 by Academic Press
All rights of reproduction in any form reserved.

TABLE 1

Analytical and Morphological Properties of the Catalysts

Sample	Nominal SO_4 (wt%)	Found SO_4 (wt%) before calcination	Found SO_4 (wt%) after calcination	Crystal phase (% t)[a] after calcination	Pt (wt%)	Surf. area ($m^2\ g^{-1}$)	SO_4 groups nm^{-2} after calcination
AZS1	6.6	6.4	6.2	100		147	2.64
AZS2	12.5	7.0	5.5	100		118	2.92
AZS3	17	nd	6.4	70		140	2.86
AZS4	22.3	14.3	9.0	30		130	4.34
PZS-A	12.3	6.8	6.1	100	0.65	140	2.73
PZS-B	12.3	7.9	6.2	100	1.06	143	2.71
PZS-C	11.7	7.2	5.8	100	4.96	145	2.50

Note. nd, not determined.
[a] t, ZrO_2 tetragonal modification.

Aerogels were obtained as follows. The wet gel, obtained according to the above procedure, was placed in a 2-liter autoclave and covered with *i*-PrOH (450 ml). After flushing with N_2, the mixture was slowly heated (2.6°C/min) up to 250°C. After stabilizing the maximum temperature and pressure (60 bar) for 1 h, the solvent was slowly removed while the temperature was slightly increased to compensate for the pressure drop. Once the solvent was completely removed, the autoclave was flushed with N_2 and cooled to room temperature.

In preparing the various AZS samples, the amount of sulfuric acid used was dosed according to the nominal SO_4^{2-} content indicated in Table 1 (second column), yielding samples that are designated AZS-*n* ($n = 1$–4) in the following. For PZS samples, the amount of sulfuric acid added was the same as that used to obtain the catalysts of the AZS2 family (see Table 1), whereas the amount of H_2PtCl_6 was dosed so as to obtain the different Pt loadings reported in Table 1 for the samples PZS-*X* (X = A–C).

As a reference material, a pure tetragonal ZrO_2 support, stabilized with 3 mol% Y_2O_3 and calcined at 600°C for 1 h (YZ samples) (12), has been loaded with the proper amount of sulfates (ex $(NH_4)_2SO_4$) and Pt (ex H_2PtCl_6) (PYZS samples) so as to obtain about the same wt% of Pt and sulfate species as present in the PZS samples. Also the parallel preparation of a non-sulfated 1 wt% Pt tetragonal ZrO_2 specimen (PYZ samples) has been carried out, and the samples have been used for comparison purposes.

After preparation by the procedures just reported, samples were calcined at 600°C for 3 h in a dry air stream (30 ml/min). After the calcination step, all samples were cooled to ambient temperature, exposed to the atmosphere, and stored in closed vessels until they were used for catalytic tests or for any of the experiments described below. Due to the rehydration brought about by exposure and storage in the air, the catalysts needed an activation (i.e., dehydration) step, which was carried out *in vacuo* for the FTIR experiments and in a dry gas stream for all other experiments.

2.2. Methods

Pt analysis was performed by AA spectroscopy. Quantitative determination of sulfates was performed by ion chromatography, and details of the experimental procedure are reported elsewhere (11). On the calcined samples, all sulfates should be considered as surface species, as after the extraction (preliminary to the ion chromatographic determination of sulfates (11)) no sulfates could be detected by IR spectroscopy in the solid residues.

BET surface areas were determined with N_2 at −196°C on a Carlo Erba 1900 Sorptomatic apparatus.

Temperature-programmed reduction with analysis by mass spectrometry (TPR–MS) was carried out in a previously described standard apparatus (13). The calcined samples were heated in 5% H_2 in Ar flow (40 ml STP/min) from 25 to 750°C at a linear rate of 10°C/min. Composition of the exit gas was monitored by injecting gas samples into a UTI 100 quadrupole mass spectrometer.

Chemisorption of H_2, CO, and O_2–H_2 titration measurements were performed in a pulse-flow system (13). Calcined samples were heated either in dry air at 450°C for 2 h (oxidative activation) or in H_2 at 300°C for 2 h (reductive activation) and then purged with Ar (or He in the case of CO chemisorption) at the same temperature for 2 h. Activated samples were then cooled in Ar (He) to 25°C to carry out the chemisorption measurement. The O_2–H_2 titration measurements were performed at 25°C by injecting pulses of O_2 on the samples after H_2 chemisorption (14).

High-resolution transmission electron microscopy (HRTEM) images were obtained with a Jeol JEM 2000 EX microscope, equipped with a top-entry stage (LaB_6 filament, 200 kV acceleration); all calcined specimens were first dispersed in *n*-heptane; then a drop of the liquid was deposited on a Cu grid coated with "holey" carbon film.

FTIR spectra were run at 2 cm^{-1} resolution on a Bruker IFS 113v spectrophotometer, equipped with an MCT

cryodetector; specimens were prepared in the form of thin layer deposition ($\sim$10 mg cm^{-2}) on a pure Si platelet, starting from an aqueous dispersion of the calcined catalysts. All thin layer samples were then thermally activated *in situ* at the chosen temperature (T/°C) in a quartz cell, equipped with KBr windows, connected to a vacuum line (final pressure $<10^{-5}$ Torr), so as to remove the abundant hydrated layer and other contaminants present on samples exposed to the atmosphere.

3. RESULTS AND DISCUSSION

3.1. Analytical and Morphological Properties

The synthetic methodology for this class of catalysts has been reported in detail elsewhere (10) and consists of a one-pot sol-gel preparation in which cogelation of $Zr(OH)_4$ with H_2SO_4 and H_2PtCl_6 is performed at room temperature in *i*-PrOH.

Evaporation of the solvent is carried out under supercritical conditions (250°C, 60 atm) leading to the formation of aerogels. The materials obtained from the evaporation step, which in most cases are already crystalline (9), underwent the calcination step at 600°C, as described under Experimental: this treatment leads to the complete crystallization of ZrO_2 and, when present, to the full reduction of the (already partly reduced) Pt component (9), in agreement with the findings of Sayari and Dicko (15). A reduction step for the Pt-containing samples was not only unnecessary for the generation of Pt metal particles, but turned out to be detrimental for the catalytic activity of the samples (9).

In Table 1, a summary of some analytical and morphological properties of the samples is shown. With the sole exception of AZS1 (whose initial sulfate loading is quite low), there is always a strong decrease in the actual amount of sulfate retained by the samples with respect to the nominal sulfate content, which corresponds to the amount of sulfuric acid introduced in the preparation.

Interestingly, the sulfate loss is quite marked even during the solvent evaporation step, as indicated by the SO_4^{2-} content measured before calcination (third column of Table 1). These materials crystallize already during the solvent evaporation step because of the high pressure, so that, in agreement with the proposal of Ward and Ko (16, 17), it can be assumed that migration of sulfate groups from the bulk of the amorphous gel to the surface of the crystalline zirconia occurs during this process. This would leave in the materials only those sulfate groups which can graft on the surface. Support for this view seems to come from an estimate of the surface concentration of sulfate groups before calcination: in most cases (the only exception is the high-loaded AZS4) the sulfate content is in the range 2.7–3.8 SO_4^{2-} groups/nm^2 (not reported in Table 1), i.e., below the statistical monolayer ($\sim$4 SO_4^{2-} groups/nm^2 (18)). The calcination step causes a further loss of sulfate, yielding materials with approximately the same sulfate content (2.5–2.9 SO_4^{2-} groups/nm^2, a figure that is far below the statistical monolayer; see last column of Table 1), still with the exception of the AZS4 system. It must be recalled that the figure giving the fraction of statistical monolayer occupied by sulfates is just a reference parameter that must be used with caution and is probably meaningful only as long as the figure remains lower than unity. In fact, the sample AZS4, whose sulfate content remains above the statistical monolayer also after the calcination step, will be shown below to possess an appreciable fraction of the surface layer that is still sulfate free.

BET surface areas of all samples, determined after the calcination step, are in the 120–150 m^2/g range (seventh column of Table 1) independently of the initial amount of sulfuric acid used.

3.2. TPR–MS

A preliminary analysis of the TPR behavior of Pt-free and Pt-promoted catalysts has already been reported in a previous paper (9). Two representative examples of TPR-MS profiles are shown in Fig. 1. All AZS samples, calcined at 600°C, display a single reduction peak starting at about 500°C with maximum centered at 680–690°C. The off-gas eluted consists essentially of SO_2 with only traces of H_2S. Conversely, PZS samples calcined at 600°C, i.e., under

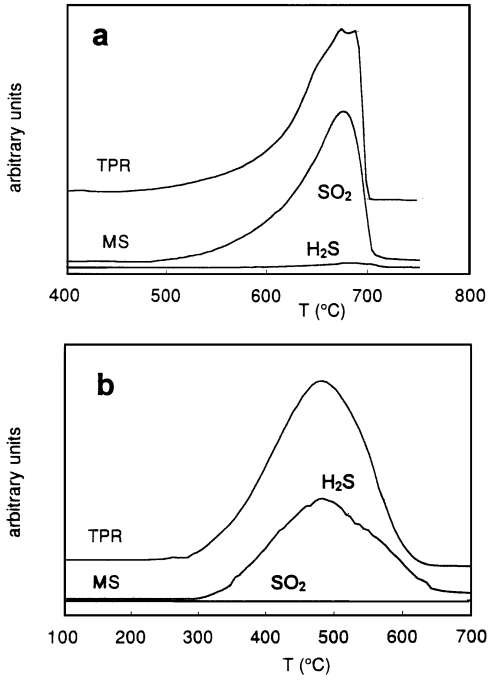

FIG. 1. TPR–MS profiles of the catalysts: (a) AZS samples; (b) PZS samples.

conditions in which Pt metal particles are fully formed (9), display a single reduction peak starting at about 300°C with maximum centered at 500°C and leading to formation of H_2S without any SO_2. This seems to suggest that the presence of the noble metal makes the reduction of surface sulfates for easier and modifies the reduction reaction(s). In all cases (both AZS and PZS samples), a quantitative determination of the H_2 consumed indicates that the sulfate groups present are completely removed during the TPR experiments.

3.3. Chemisorption

Chemisorption data are reported in Table 2. Hydrogen chemisorption was measured on all of our Pt-containing catalysts following the procedure reported under Experimental. Under these conditions H/Pt values of ~0.2 were observed for PZS-A and PZS-B, whereas for the high-loaded PZS-C the H/Pt value decreased to 0.11. A mild reductive treatment (300°C) prior to hydrogen chemisorption suppressed completely the chemisorption capacity of all catalysts, whereas a (virtually) complete recovery was observed after an oxidative treatment at 450°C. Reduction/oxidation cycles could be repeated several times, as indicated in Table 2 in the case of PZS-B, with only minor changes in the hydrogen chemisorption properties.

After hydrogen chemisorption, titration with O_2 at 25°C was performed. The amount of oxygen consumed was found to be very small in all cases, and in the case of the low-loaded PZS-A reliable figures could not be obtained. In the other cases (see Table 2), O/Pt values of 0.026 and 0.039 were observed, leading to O/H experimental ratios of 0.13 and 0.35, respectively, at variance with the expected theoretical ratio of 1.5. This observation seems to suggest that much of the hydrogen consumed by the catalysts during the chemisorption experiments undergoes spillover to the support and that only a minor fraction remains actually chemisorbed on platinum.

Finally, chemisorption of CO at 25°C was performed on all catalysts, although again only PZS-B and PZS-C gave reliable figures (see last column of Table 2). After an oxidizing treatment, i.e., under the condition in which the catalysts are able to chemisorb hydrogen, a CO/Pt ratio of 0.075 and 0.033 was observed. A reductive treatment was observed to reduce the adsorption capacities of the catalysts, and new CO/Pt values of 0.020 and 0.011 were observed, respectively.

The reduced capacity to chemisorb CO after a reductive treatment parallels the behavior observed for hydrogen chemisorption. Since the phenomena induced on the catalysts by the reductive treatment have to be the same in both cases, one must conclude that CO is adsorbed also on surface sites other than Pt, so as to explain the ability of the catalysts to retain an appreciable residual capacity to chemisorb CO. If the amounts of CO chemisorbed are expressed per gram of catalyst, the figures corresponding to PZS-B and PZS-C after the oxidative treatment are 0.092 and 0.073 ml g^{-1}, respectively, even though the Pt content of the two catalysts is very different. It can be reasonably assumed that much of the CO is adsorbed by surface Zr^{4+} Lewis acid sites produced upon thermal dehydration (the activation step), as confirmed by the IR experiments (*vide infra*).

The observation that a reductive treatment strongly decreases the CO chemisorption capacities and completely suppresses the hydrogen chemisorption capacities is surprising and suggests that part of the surface sulfates can be reversibly reduced in the presence of Pt to a strongly bound form of sulfur (for example, sulfide). This would mask completely the Pt surface toward hydrogen and CO chemisorption, so that the latter probe molecule can adsorb only on strong Lewis Zr^{4+} centres. This "reduced sulfur" species on Pt would be promptly reoxidized to sulfate by oxygen, as demonstrated by the fact that the hydrogen chemisorption capacities can be recovered indefinitely by an oxidative treatment.

In general, however, the uptake of oxygen, i.e., of the only gas that can be reasonably assumed to titrate selectively the available Pt centers, is exceedingly low. If the net oxygen uptake by Pt is used to calculate the average metal particle size, diameters of 80 and 43 nm are obtained for PZS-B and PZS-C, respectively. Since the average sizes determined by X-ray diffraction (9) and confirmed below by TEM data are actually 10.3 and 15.4 nm, respectively, it must be concluded that, even in the merely calcined samples, the Pt surface is chemically shielded so that only a small fraction of the potential surface Pt centers are available for chemisorption. It seems reasonable to propose that what hinders the Pt surface are some of the surface sulfate groups grafted on ZrO_2, shielding appreciable portions

TABLE 2

Summary of the Chemisorption Properties of the PZS Samples

Sample	Pretreatment[a]	H/Pt	Total O/Pt[b]	O/H	Net O/Pt[c]	CO/Pt
PZS-A	oxidative	0.186				
PZS-B	oxidative	0.203	0.026	0.13	0.017	0.075
PZS-B	reductive	0				0.020
PZS-B	oxidative	0.191				
PZS-B	reductive	0				
PZS-B	oxidative	0.187				
PZS-C	oxidative	0.112	0.039	0.35	0.026	0.033
PZS-C	reductive	0				0.011

[a] Oxidative pretreatment: 2 h at 450°C in air; reductive pretreatment: 2 h at 300°C in hydrogen. In both cases, after the pretreatment, samples were cleaned in a stream of argon at the same temperature of the pretreatment.

[b] Total oxygen uptake by the samples including oxygen consumed to titrate chemisorbed hydrogen.

[c] Net oxygen chemisorbed by Pt.

of the Pt particles. These are most likely to be the sulfate groups that are reduced (leading to complete masking of Pt) and reoxidized by Pt (yielding back the chemisorptive capacity of Pt) during the reversible reduction/oxidation cycles. Indeed, analytical data of Table 1 and the Pt and ZrO_2–SO_4 crystallite size dimensions determined by X-ray diffraction analysis (9) indicate that in PZS samples the ratio between the number of ZrO_2–SO_4 and Pt particles is approximately in the range 700–1500. Since Pt particles are generally larger than ZrO_2–SO_4 particles (from X-ray analysis, 6.5–15.4 nm vs 5–8 nm (9)), a common occurrence is likely to be that of a Pt particle bearing in close proximity (or even being surrounded by) a number of ZrO_2–SO_4 particles. This view could well explain an extensive Pt–SO_4 interaction and the poor oxygen and CO chemisorption properties of Pt in these samples.

3.4. HRTEM Characterization

HRTEM images of some AZS, PZS, PYZS, and PYZ samples are reported in Fig. 2. The samples were examined "as obtained," i.e., after the preliminary calcination step at 600°C. The low-loaded Pt sample (Fig. 2a: PZS-A, 0.5 wt%) shows the typical morphological features of a high-surface area (sulfated) zirconia system, made up of small flat crystallites (5–8 nm), whose top termination is quite regular (as demonstrated by sharp interference fringe patterns and frequent moiré fringes) and whose stepped and often roundish contours indicate the highly defective nature of the side terminations. In the low-loading PZS-A system there is no occurrence of visible metallic Pt aggregates or islands. This observation is in apparent contradiction with XRD data reported in a previous note (9), where after calcination a

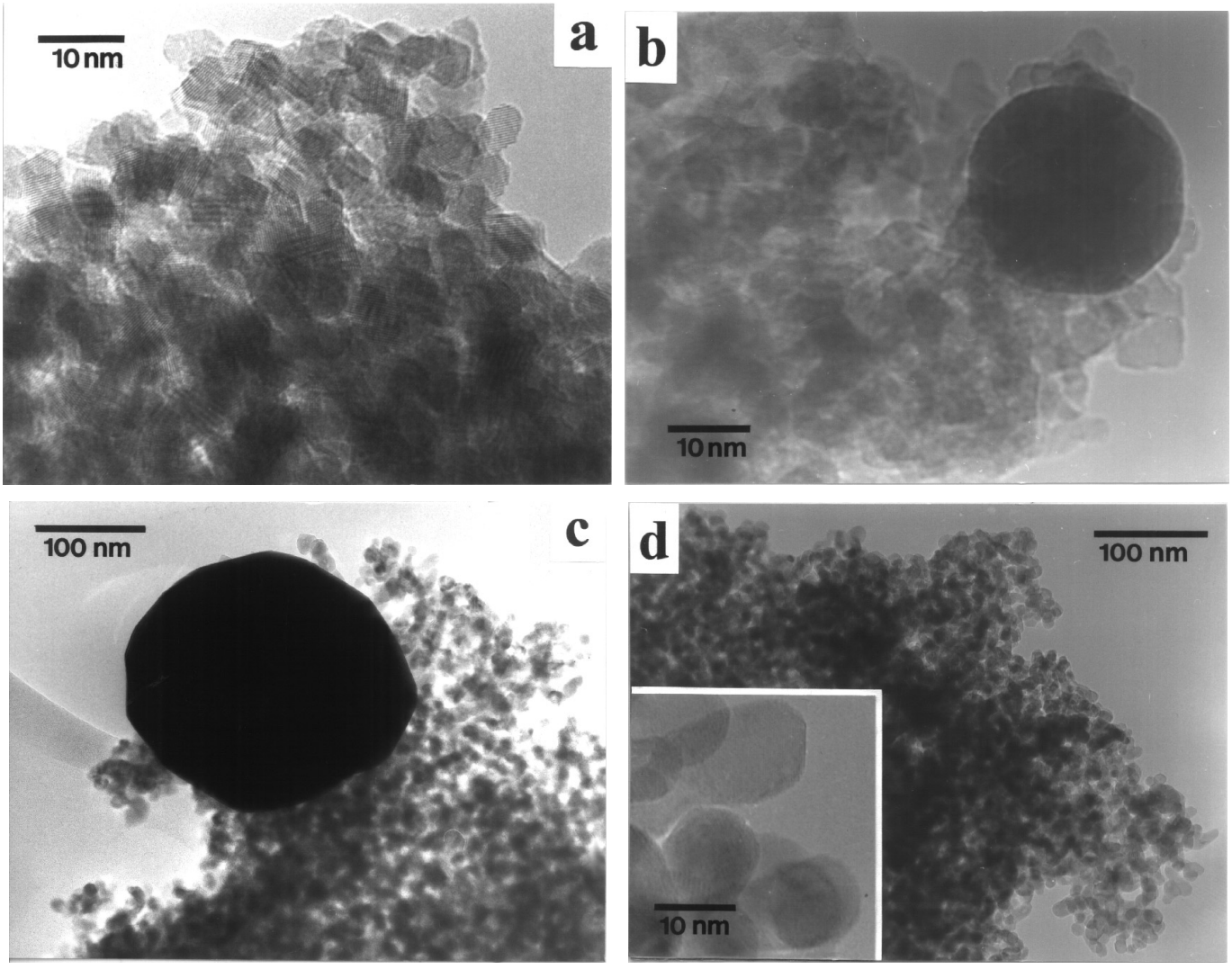

FIG. 2. HRTEM images of the catalysts: (a) PZS-A (0.53 wt% Pt) and AZS2 (no Pt); (b) PZS-C (5 wt% Pt); (c) PZYS (1 wt% Pt); (d) PYZ (no sulfates; 1 wt% Pt).

shallow peak at $2\theta \approx 40°$, ascribable to the Pt(111) reflection (19), indicated the presence of Pt particles of ∼65 Å diameter. The size of these Pt particles is definitely larger than the usual size of Pt in other well-known catalysts of similar Pt concentration (e.g., 0.5 wt% Pt on alumina yields normally particles of ∼10–30 Å) and should be observable in the (HR)TEM mode.

On the high-loaded Pt system (Fig. 2b: PZS-C), typical ZrO_2 particles are still observable with virtually unchanged characteristics, meaning that forming crystalline ZrO_2 in the presence of a large amount of Pt does not appreciably affect the morphological evolution of the ZrO_2 system. Pt aggregates are now well visible, as fairly large crystallites of metallic Pt (∼20 nm diameter) can be seen in samples that did not undergo any reductive treatment. This is consistent with what has already been reported in the X-ray analysis of these samples (9) and confirms a moderate dispersion of Pt on sulfated ZrO_2.

It is possible that the presence of sulfates is actually responsible for the unusual morphological characteristics of the Pt-on-ZrO_2 species, and to confirm this hypothesis a parallel morphological investigation should be carried out on a nonsulfated Pt-on-ZrO_2 system. However, in the case of the standard PZS catalysts this comparative approach is not possible, because the absence of sulfate species would lead, during the calcination step at 600°C, to monoclinic ZrO_2. Indeed, monoclinic and tetragonal ZrO_2 are known to behave quite differently; for instance, sulfated monoclinic ZrO_2 normally exhibits negligible catalytic activity (20). To overcome this difficulty, we have resorted to the sample termed PYZS: this is a reference preparation of Pt-promoted sulfated tetragonal ZrO_2 stabilized with Y_2O_3, for which the nonsulfated counterpart exists (the system termed PYZ) and is stable.

Figure 2c reports the morphological features of PYZS. It is evident that in this case the aggregation of Pt particles has occurred to an even more abnormal extent, as large aggregates of metallic Pt of average diameter ∼80–150 nm (i.e., much larger than in the case of PZS) are observable. (Note that the Pt particle shown in Fig. 2c is the largest one observed, but very few Pt particles were found to have diameter below 120 nm.) This observation is consistent with what is reported in the literature: supported Pt tends to aggregate much more easily in the presence of surface anionic species (21).

The morphological features of the nonsulfated PYZ system are shown in Fig. 2d. Both before and after a reductive treatment in H_2 there is no evidence for Pt aggregates, as the TEM images are those observable also with a plain yttria-stabilized tetragonal zirconia: flat crystallites of ∼10–15 nm size, mostly iso-oriented along the (111) direction of tetragonal ZrO_2, and with roundish (i.e., crystallographically defective) contours. It is thus confirmed that, in supported Pt systems, the agglomeration of Pt tends to proceed quite rapidly in the presence of foreign anionic species.

3.5. FTIR Spectra

3.5.1. Background Spectra of Sulfate Species

A. Activation at $T < 500°C$ (AZS2 and PZS samples). Figure 3 reports the spectral features of surface sulfate groups as a function of the thermal dehydration temperature (the activation step). One typical spectral pattern summarizes the behaviour of all PZS catalysts and of the parent AZS2 samples. (Only the samples of the AZS4 family behave somewhat differently, and these are dealt with separately in the next section.)

The presence of Pt does not affect the structure and thermal behavior of sulfates (22), as long as the activation temperature is kept below 500°C. Moreover, no appreciable differences between AZS2 and PZS systems are observed for $T_{act} < 500°C$ also when the treatment is carried out in the presence of H_2 (reductive treatment).

The spectra are characterized by the presence of absorptions due to the S=O and S–O vibrations of sulfates; these modes are well known and have been discussed, for instance, in Ref. (23). In high hydration stages (curve 1 of Fig. 3), surface sulfates possess an *ionic structure*, characterized by a broad band in the 1300–1200 cm^{-1} region and a complex band envelope in the 1200–950 cm^{-1} spectral range (24a). Another broad band envelope is present at

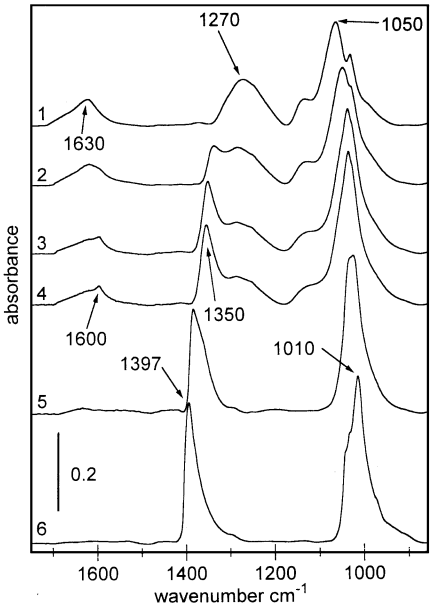

FIG. 3. FTIR spectra (for absorbance units, see inset vertical line; 1750–850 cm^{-1} range) of AZS and PZS catalysts. (1) catalyst "as is," in air; (2) vacuum evacuated at room temperature (RT) for 10 s; (3) activated *in vacuo* at RT, for 5 min; (4) RT, for 1 h; (5) 200°C; (6) 400°C. The spectra do not change to an appreciable extent if these thermal treatments are carried out in an H_2 atmosphere.

$\sim$1630 cm^{-1} ascribable to the bending mode (δ_{HOH}) of water molecules physisorbed and/or coordinated at the surface (24). With proceeding dehydration (curves 2–6 of Fig. 3), there is the gradual transformation of sulfates into a *covalent structure* (25), characterized by a sharp band positioned at 1350–1400 cm^{-1}, ascribable to the (asymmetric) $\nu_{S=O}$ stretching mode, and by a band envelope centered at 1050–1000 cm^{-1}, ascribed to the ν_{S-O} stretching.

Parallel to the transformation of sulfates, the early stages of dehydration bring about the modification and, eventually, the disappearance of the broad band ascribed to the δ_{HOH} mode of adsorbed water. For instance, curve 4 of Fig. 3 shows that this band declines and becomes more resolved on its low ν side, revealing at $\sim$1600 cm^{-1} a sharp band that was previously ascribed to the δ_{HOH} mode of a quasi-free H_3O^+ species (25). The presence of the sharp band at $\sim$1600 cm^{-1} is thought to be the spectral monitor of the residual presence at the surface of hydrated protonic acid centers (hydrated Brønsted sites) and is typical of sulfated zirconia catalysts that, *when dehydrated at* $T_{act} \approx$ *400°C*, are catalytically active for the isomerisation of *n*-alkanes. The sharp band at $\sim$1600 cm^{-1} declines at $T_{act} = 150$°C and is eliminated *in vacuo* at $T_{act} = 180$–200°C. While this paper was being reviewed, an alternative interpretation was proposed for the sharp band at $\sim$1600 cm^{-1} (38): it would be the overtone of an OH bending mode occurring at about 850 cm^{-1}. This assignment is rather unconvincing, as it is hard to accept that one can easily observe the sharp overtone of a fundamental mode that cannot be singled out in the background spectrum (note that with our thin-layer samples and IR cells with KBr windows, the background spectrum can be examined down to $\sim$780 cm^{-1}). Moreover, it is hard to accept that a surface OH group is rapidly eliminated at 150–180°C and is readily restored upon water uptake (25).

It is important to recall here that all PZS and AZS specimens develop their catalytic activity toward *n*-butane isomerization *only* when sulfate groups reach the covalent configuration, i.e., for $T_{act} = 400$–450°C, a temperature necessary to bring the surface to a medium-high dehydration stage (25). Moreover, as was anticipated in previous work (20, 26), the best catalytic performance of sulfate-doped ZrO_2 (either promoted with Pt or nonpromoted) is observed when in the IR spectrum of the covalent sulfate species the sharp $\nu_{S=O}$ band at $\sim$1400 cm^{-1} and the low-lying ν_{S-O} band centered at $\sim$1010 cm^{-1} reach their (relative) maximum intensity. For instance, curve 6 of Fig. 3 reports the typical spectrum of a sulfated ZrO_2 system (with or without Pt) that, through proper calcination (at $T_{calc} > 500$°C) and activation treatments (at $T_{act} = 400$–450°C), reached a good catalytic activity (26). Any thermal and/or chemical treatment which leads to the decline or disappearance of the sulfate spectral components mentioned above implies the almost irreversible decline of activity or deactivation of the catalyst, because no further treatment (except, perhaps, a further sulfation step) would be able to restore the relevant sulfate species and the catalytic activity therefrom.

B. Activation at T < 500°C (AZS4 samples). The samples termed AZS4 deserve a brief separate comment. The main peculiarity of these catalysts resides in the fact that they retain, also after the calcination step at 600°C, a high surface sulfate content (above a statistical monolayer) and that the crystal structure of the resulting ZrO_2 phase is over 70% monoclinic. Moreover, unlike what has been observed so far with most monoclinic sulfated ZrO_2 systems calcined (at 600°C) and activated (at 400°C), the catalysts of the AZS4 family turn out to be catalytically active, as will be described in detail in Part 2 of this work.

Nevertheless, the unusual behavior of AZS4 systems *does not* contradict what has been stated in the previous section on the correlation between catalytic activity and spectral features of surface sulfates. In fact, Fig. 4a shows that, even though the overall shape of the background spectrum of AZS4 (curve 2) is rather different from that of the tetragonal system AZS2 (curve 1), the ν_{SO} bands at $\sim$1400 and $\sim$1010 cm^{-1}, ascribed to "active" surface sulfates, are strong and predominant also in the case of the AZS4 system.

This observation is at variance with what has been reported previously for the sulfates of monoclinic sulfated ZrO_2 systems (23, 27) obtained by direct sulfation of either a crystalline monoclinic ZrO_2 preparation or a crystalline metastable (i.e., nonstabilized) tetragonal ZrO_2

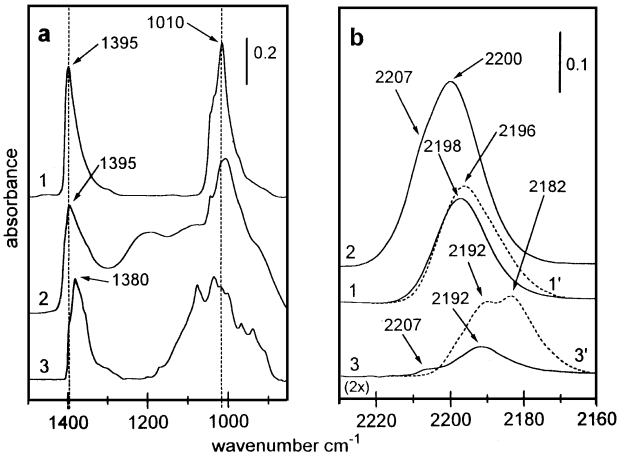

FIG. 4. (a) FTIR spectra (absorbance units, inset; 1500–850 cm^{-1} range) of the sulfates at the surface of some sulfated ZrO_2 samples, after vacuum activation at 400°C. (1) AZS2; (2) AZS4; (3) ZRP [3.3H] (see Ref. (11); solid is pure monoclinic ZrO_2, sulfate-loaded (3.3 SO_4^{2-} groups per nm^{-2}) by direct contact with H_2SO_4). (b) FTIR spectra (absorbance units, inset; 2230–2160 cm^{-1} range) relative to the RT adsorption of 100 Torr CO onto various ZrO_2 samples, vacuum activated at 400°C. (The numbering of the CO spectra corresponds to that of the sulfate spectra in Section 4a). (1) AZS2; (1′) YZ (sulfate-free tetragonal ZrO_2); (2) AZS4; (3) ZRP [3.3H], i.e., sulfated pure monoclinic ZrO_2 (curve 3 underwent a twofold ordinate expansion); (3′) ZRP, i.e., sulfate-free pure monoclinic ZrO_2.

preparation. In fact, curve 3 of Fig. 4a shows that, in these latter cases, the spectrum of surface sulfates is quite different and, in particular, the ν_{SO} bands at ~1400 and ~1010 cm^{-1}, ascribed to "active" surface sulfates, are very scarce. Figure 4b, concerning the adsorption of CO on the samples presented in Fig. 4a, will be discussed in a following section.

C. Activation at $T > 500°C$ (AZS2 and PZS samples). When the thermal treatments, either *in vacuo* or in hydrogen, are carried out at temperatures higher than 500°C, the description of the spectral features of sulfates has to be carried out separately for AZS and PZS catalysts, because of their different behavior.

Figure 5 reports the behavior of the typical Pt-free system AZS2. Surface sulfates of AZS systems are thermally stable in the 400–550°C range (see curves 1 and 2 in Fig. 5a), as the strong $\nu_{S=O}$ band at ~1396 cm^{-1} and the corresponding ν_{S-O} component at ~1010 cm^{-1} maintain a constant profile. For vacuum treatments at higher temperatures, surface sulfates decline: they decline slightly for $T_{act} = 600°C$ (see curve 3), whereas they are almost completely eliminated when T_{act} reaches 700°C (see curve 4 in Fig. 5a). Note, in particular, that the catalytically important components at ~1400 and ~1010 cm^{-1} tend to be eliminated first.

When the thermal treatment of AZS-2 was carried out at 500°C in a reducing atmosphere, followed by outgassing at the same temperature to maintain the starting dehydration degree (see curve 2red in Fig. 5b), an appreciable decline of intensity and an altered spectral shape of surface sulfates were observed: the residual $\nu_{S=O}$ mode became positioned at lower frequency (~1370 cm^{-1}), and in the ν_{S-O} band envelope the low-frequency component (~1010 cm^{-1}) disappeared almost completely. The stability toward reduction of sulfates of AZS systems was also anticipated by TPR–MS experiments, in which H_2 consumption was evident at $T > 500°C$ (see Section 3.2), with the predominant detection of a fragment of mass 64 amu, indicative of SO_2 production. In addition to this, IR data show that the elimination by reduction of the various sulfate species is selective, as the "active" sulfates absorbing at ~1400 and ~1010 cm^{-1} are eliminated first.

After reduction, a subsequent treatment in an oxidizing atmosphere (curve 2ox in Fig. 5b) does not reproduce the original spectral features of sulfates. In fact, the catalytically important spectral components at ~1400 and ~1010 cm^{-1} remain almost absent, whereas a new absorption is now present at ~925 cm^{-1}. The latter may be tentatively ascribed to the ν_{SO} stretching of an SO_x species, in which the sulfur atom possesses a valence state lower than 6, as, for instance, in sulfite species (28).

To summarize this section:

(i) surface sulfate species of AZS catalysts are thermally stable in the 30–550°C interval, in which they reach and maintain the so-called *covalent structure*, with parallel developing of their best catalytic performances;

(ii) for vacuum activation at temperatures up to 700°C, or for thermal treatment in H_2 atmosphere at up to 500–600°C, there is the gradual and irreversible destruction of "active" sulfate species, and the parallel decline of catalytic activity;

(iii) the thermal and/or chemical (reductive) elimination of sulfates leads mostly to the production and evolution of SO_2, so that a further oxidative treatment is unable to restore the starting amount of surface sulfur-containing species and, probably, the +6 state of sulfur.

Unlike AZS systems, in the presence of Pt (PZS samples), sulfate groups start to decline thermally very fast, and they are completely eliminated after a vacuum activation at ~600°C (see curves 1–3 in Fig. 6a). Already after a thermal treatment at intermediate temperatures (i.e., vacuum activation at 500°C; see curve 2), there is an appreciable elimination of sulfates and, in particular, of the "active" sulfate species (~1390 and ~1010 cm^{-1}). In fact, the maximum of the residual $\nu_{S=O}$ mode shifts to lower frequency (1377 cm^{-1}) and the ν_{S-O} mode envelope loses selectively its low-frequency component (~1010 cm^{-1}).

If the thermal treatments are carried out in a reducing atmosphere, the tendency of Pt-containing systems to lose their surface sulfate species more easily than Pt-free systems is confirmed. In fact curve 2red in Fig. 6b shows that treating PZS-B at 500°C in H_2 eliminates more sulfates than a plain vacuum activation at the same temperature on both AZS (curve 2 of Fig. 5a) and PZS (curve 2 of Fig. 6a). A subsequent thermal oxidizing treatment is able to restore

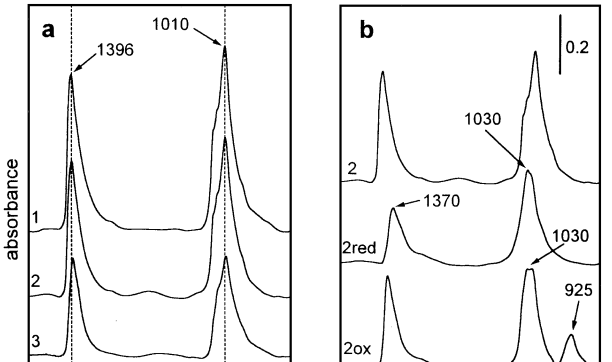

FIG. 5. FTIR spectra (absorbance units, inset; 1500–850 cm^{-1} range) of AZS2 catalysts activated at increasing temperatures, either *in vacuo* or in the indicated atmosphere. (a) Different thermal treatments carried out *in vacuo*: (1) $T_{act} = 400°C$; (2) $T_{act} = 500°C$; (3) $T_{act} = 600°C$; (4) $T_{act} = 700°C$. (b) AZS2 after the following treatments: (2) *in vacuo* at 500°C (same as trace 2 of (a)); (2red) in reducing atmosphere at 500°C; (2ox) reduction (2red) followed by oxidizing atmosphere at 500°C.

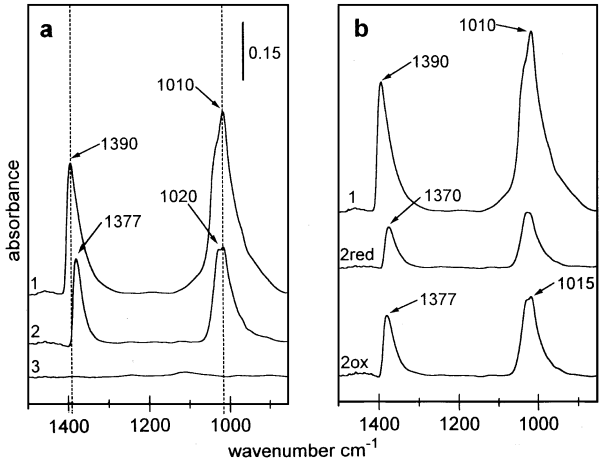

FIG. 6. FTIR spectra (absorbance units, inset; 1500–850 cm^{-1} range) of PZS-B (1 wt% Pt) catalysts activated at increasing temperatures, either *in vacuo* or in the indicated atmosphere. (a) Different thermal treatments carried out *in vacuo:* (1) $T_{act} = 400°C$; (2) $T_{act} = 500°C$; (3) $T_{act} = 600°C$. (b) PZS-B after the following treatments: (1) *in vacuo* at 400°C; (2red) in reducing atmosphere at 500°C; (2ox) reduction (2red) followed by oxidizing atmosphere at 500°C.

an appreciable fraction of surface sulfates, corresponding to ∼50% of the starting amount (compare the three curves in Fig. 6b). This indicates that an appreciable fraction of reduced sulfur did *not* evolve from the sample but remained, after reduction, bound in the sample. However, two comments are important: (i) although in the oxidation step more sulfates are restored than in the case of AZS systems, also on Pt-promoted systems the typical $\nu_{S=O}$ and ν_{S-O} components associated with the best catalytic performances are not restored and, in fact, the catalytic activity turns out to recover only to a minimal extent; (ii) the spectrum 2ox of Fig. 6b is virtually identical to spectrum 2 of Fig. 6a meaning that, at 500°C, the sulfate destruction effect achieved on Pt-containing catalysts by a vacuum thermal treatment is the same as can be achieved through a reduction/oxidation cycle.

It is important to recall that TPR data (Section 3.2) showed that, in the early 300–550°C thermal range of PZS, there is a broad peak due to H_2 consumption, which agrees well with the early elimination of sulfate groups monitored by IR spectroscopy. Parallel to that, MS data indicated that the fragment detected could be attributed mainly to H_2S (*m/z*: 34 amu).

A possible mechanism that might be proposed to explain the data presented here is as follows:

(i) in the presence of Pt, reduction of sulfates to sulfides (rather than to SO_2) prevails in the 450–550°C thermal range: $S^{6+} \rightarrow S^{2-}$;

(ii) part of the sulfide species formed by reduction may interact with Pt species, to give, for instance, PtS (29): in this way, not all of the reduced sulfur is removed from the surface of the catalyst;

(iii) surface sulfides may be then reoxidized to sulfates. However, unfortunately, the family of the "active" sulfate species connected with the good catalytic activity (monitored, for instance, by the ν_{S-O} band at ∼1010 cm^{-1}) is not restored at all. This means that, when the elimination of the "active" sulfates is achieved (either by thermal decomposition or by reduction), the relevant sulfur is not fixed by the catalyst and the removal is irreversible.

3.5.2. Adsorption of CO at Room Temperature

In order to test spectroscopically the surface Lewis acidity that develops on the ZrO_2 moiety upon dehydration (i.e., in the activation step (24b)), and the adsorption capacity of supported Pt we have performed the adsorption of carbon monoxide (CO) at room temperature (RT).

CO adsorption at RT is a suitable surface probe (27, 30), due to its high selectivity in revealing: (i) strongly uncoordinated (c.u.s.) surface cationic sites (Zr^{4+}), forming weak σ-dative complexes characterized by ν_{CO} frequencies higher than that of the free CO gaseous molecule (2143 cm^{-1}), the upwards shift of the ν_{CO} band of these σ-complexes paralleling the Lewis acidity of the sites; (ii) the presence of coordinative vacancies on surface metal atoms, forming strong σ–π complexes, characterized by ν_{CO} frequencies lower than that of the free CO gaseous molecule.

Through the RT adsorption of CO, Fig. 4b reports the surface situation presented by some of the Pt-free sulfated ZrO_2 systems of interest. (It is recalled that the corresponding Fig. 4a was mainly devoted to the peculiar behavior of the mostly monoclinic AZS4 systems, as compared with the other tetragonal AZS systems.) Curve 1 of Fig. 4b corresponds to the adsorption of CO (100 Torr) onto c.u.s. Zr^{4+} centers at the surface of AZS2 (tetragonal system), rendered catalytically active by vacuum activation at $T_{act} = 400°C$. The comparison of the CO band at ∼2198 cm^{-1} with the corresponding dotted-line band of curve 1′ (∼2196 cm^{-1}), due to CO uptake onto the sulfate-free tetragonal system YZ indicates that, on active tetragonal catalysts: (i) sulfates do not occupy all of the surface Zr^{4+} sites at which CO can adsorb at RT; (ii) the presence of sulfates modifies only slightly, by inductive effects, the Lewis acidity of c.u.s. Zr^{4+} centers. In fact, an upwards ν_{CO} shift of a few wavenumbers corresponds to a modest increase of acidic strength.

Curve 2 of Fig. 4b presents one more aspect of the peculiar behavior of AZS4: although the concentration of sulfates on the calcined system is slightly above that of a statistical monolayer (4.34 vs ∼4 groups per nm^2), a substantial amount of c.u.s. Zr^{4+} surface sites capable of chemisorbing CO are accessible. This means that in the part(s) of the surface occupied by sulfates, sulfates tend to assume a structure that is more complex and less space consuming than that corresponding to a regular SO_4^{2-} ion (18). The formation of complex sulfates at the surface of monoclinic ZrO_2 when

the sulfate loading becomes high has also been suggested by other authors (23). Moreover, the comparison of the complex CO band of curve 2 with the dotted-line trace of curve 3′, corresponding to CO adsorbed on a sulfate-free monoclinic ZrO_2, indicates that in the case of monoclinic ZrO_2 the inductive effects from surface sulfates are felt quite strongly by nearby c.u.s. Zr^{4+} sites, as the upwards ν_{CO} shift is of some 10–15 cm^{-1} (27, 31). Such a shift indicates a substantial increase of Lewis acidic strength. In particular, the main difference between the (mostly monoclinic) AZS4 catalyst and "regular" (tetragonal) catalysts like AZS2 resides in the presence, on the former, of a substantial amount of very strong Lewis sites ($\nu_{CO} \approx 2208\ cm^{-1}$), which are not present on the latter: this peculiarity will be correlated in Part 2 with an unusual reactivity behavior of the AZS4 systems.

Turning now to the systems promoted with Pt, it is worthwhile recalling that the RT adsorption of CO on surface-exposed Pt should bring about the formation of various CO adspecies (linear or bridged complexes), whose ν_{CO} stretching modes absorb in the 2150–2040 cm^{-1} and in the 1820–1870 cm^{-1} ranges, respectively (32). In the case of the far more frequent and abundant linear CO complexes, the ν_{CO} frequency is indicative of the oxidized/reduced state achieved by Pt: a ν_{CO} frequency at ~2080–2100 cm^{-1} is normally thought to be indicative of a linear carbonyl complex formed on metal Pt particles, (see, for instance, Ref. (32), concerning CO adsorption on single crystal and/or supported Pt^0 species), whereas a ν_{CO} mode absorbing at ~2130–2150 cm^{-1} is thought to imply the formation of Pt^{n+}–CO adspecies (33).

Figure 7 reports the spectral features relative to the adsorption of CO at room temperature onto PZS-B catalysts, and onto a PYZ catalyst used as a reference system (top curve, numbered 5).

After a vacuum activation at $T_{act} = 300$–450°C (we recall that this is the temperature range needed to activate, either *in vacuo* or in inert gas, the catalysts before the catalytic reaction to be run at 150–250°C (34), and is also the activation temperature used before testing the surface reactivity by FTIR spectroscopy), no difference is observed for CO interaction with either AZS2 or PZS specimens, indicating that the same kind of activity toward CO has developed at the surface of either Pt-promoted or nonpromoted sulfated ZrO_2.

For this reason we have reported only one spectrum (curve 1 of Fig. 7) to represent the behaviour of CO on both systems. Only one carbonyl component is present at ~2200 cm^{-1}, ascribable to c.u.s. Zr^{4+} cations (strong Lewis sites) present abundantly in this medium-high dehydration step, and located in crystallographically defective configurations (3, 4, 26). No bands due to Pt–CO interaction are evident, and this observation is in agreement with previous literature data (34) and with what is reported in the chemisorption section (Section 3.3) for PZS systems reduced in H_2.

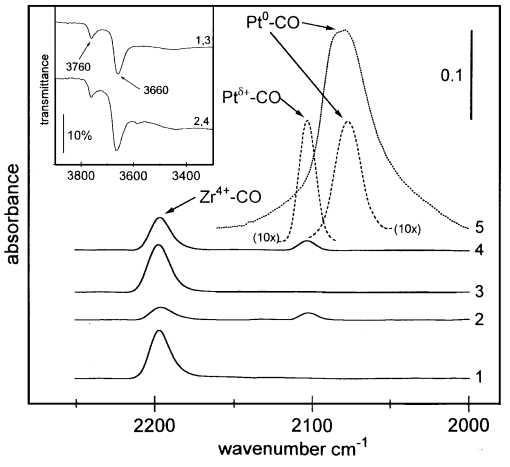

FIG. 7. FTIR spectra (absorbance units, inset; 2250–2000 cm^{-1} range) relative to the RT adsorption of 100 Torr CO onto a PZS-B (1 wt% Pt) sample, activated *in vacuo* at 300°C (curves 1 and 3) and further oxidized with O_2 at 300°C (curves 2 and 4; after oxidation, the samples were evacuated (to remove O_2) only after cooling to room temperature). Curve 5 represents CO adsorbed in the same conditions onto the reference nonsulfated PYZ sample (1 wt% Pt) reduced at 300°C. Inset: OH spectra pattern (percent transmittance; 3900–3300 cm^{-1} range) of the PZS-B sample (the numbering corresponds to that of the rest of the figure).

Most surprisingly, Pt–CO species start to be revealed only after a subsequent treatment of the catalyst in an *oxidizing* atmosphere. Curve 2 in Fig. 7 and the magnified broken-line traces above curve 4 show that, under these conditions, a weak band is formed, absorbing either at ~2100 cm^{-1} or at ~2080 cm^{-1}. The frequency at which this CO band occurs is unpredictable and is indicative of a variable and unpredictable oxidation state of the surface Pt. A CO band at ~2100 cm^{-1} is ascribable to Pt^0–CO species in an oxidized Pt system, whereas a band at ~2080 cm^{-1} is indicative of a Pt^0–CO species in a reduced Pt system (32d, 33c). According to literature data (10, 36) and to our observations in Section 3.1, Pt ions are partly transformed into metallic Pt particles during supercritical evaporation of the solvent and completely during the calcination step; even so, after the first vacuum activation step (curve 1), no CO/Pt interaction is detected, and this suggests that the mildly reducing ambient of a vacuum activation at 300–400°C is sufficient to achieve the same shielding of surface Pt centers as is achieved in a reducing atmosphere at 300°C. When, after the oxidation step, a CO/Pt interaction starts to become observable (in agreement with the data relative to H_2/O_2 chemisorption reported in Section 3.3), the intensity of the Pt^0–CO band turns out to be almost negligible (33) if compared with that obtained, under the same conditions, for the nonsulfated PYZ (1 wt% Pt) reference sample (compare curves 2, 4 and 5 in Fig. 7).

These facts indicate that: (i) on the catalysts activated *in vacuo*, Pt particles become in some way completely shielded

by surface species, such as, for instance, sulfates, sulfides, and/or hydrides; (ii) Pt species supported on a sulfated surface tend to form medium-large aggregates (also partly interacting with sulfates or other surface species), so that when Pt surface sites become available for CO chemisorption, the extent of this interaction is very scarce.

The activation treatment at 300–400°C eliminates most of the abundant hydrated layer present at the surface of the starting (calcined) catalysts and yields a well-defined OH pattern, consisting of two different free OH species of odd intensity, ascribed to terminal OH and (tri)-bridged surface OH, respectively (17, 37) (see curve 1 in the inset to Fig. 7). The oxidative treatment, which permits the adsorption of carbon monoxide onto Pt species, implies a partial rehydration of the surface (due to the burn-off of hydrogen-containing surface species, e.g., surface hydrocarbonaceous contaminants always present in a conventional vacuum system). This is monitored by: (i) the much lower intensity of the Zr^{4+}–CO component (curve 2 in Fig. 7); (ii) the spectra in the ν_{OH} region, altered by the presence of new OH species interacting by H-bonding (see curve 2 in the inset to Fig. 7); (iii) the spectral position of the $\nu_{S=O}$ and the ν_{S-O} modes of sulfates, which become located at lower and higher frequencies, respectively (not reported for the sake of brevity), due to a partial ionic configuration of surface sulfate species brought about by partial rehydration.

If the oxidized PZS sample is reactivated *in vacuo* at 300–400°C, its spectral features recover the starting shape: in particular, the Zr^{4+}–CO band recovers the initial ν_{CO} frequency and intensity (the sample has dehydrated again), and, again, no Pt^0–CO component is evident in the spectrum any longer (curve 3 in Fig. 7); Pt sites have been shielded again, as in the case of a reduction in H_2 at 300°C. This activation/deactivation pattern can be reproduced indefinitely: after a further oxidative treatment at 300–400°C, followed by contact with CO at ambient temperature, the spectrum will present the same features as are evidenced after the first activation in O_2 (compare, for instance, curves 2 and 4 in Fig. 7; also in this case, the position of the CO/Pt band is variably located between 2080 and 2100 cm^{-1}.

4. CONCLUSIONS

The data presented and discussed in this work allow the following conclusions to be made:

(i) The one-pot preparation procedure adopted here yields sulfated zirconia specimens that are mainly tetragonal for starting H_2SO_4 content below ∼20 wt%, and mainly monoclinic for H_2SO_4 content above ∼20 wt%. This is quite unexpected, and even more unexpected is the fact that the mainly monoclinic sulfated ZrO_2 systems retain a sulfate content above that of a statistical monolayer and are catalytically active.

The catalytic activity of these mainly monoclinic systems is consistent with the presence, on the dehydrated samples, of abundant covalent sulfates absorbing at ∼1400 and ∼1010 cm^{-1}: these frequencies are typical of the family of covalent sulfates present on all active tetragonal sulfated ZrO_2 systems (both Pt-free and Pt-promoted). In contrast, sulfates absorbing at these frequencies are normally scarce on monoclinic sulfated ZrO_2 systems obtained by other methods and are largely inactive.

The reasons that the presence of a large amount of starting H_2SO_4 in the sol-gel preparation step leads to atypical monoclinic sulfated ZrO_2 are still not understood.

(ii) In the sulfated ZrO_2 systems containing Pt, the solvent evaporation step brings about an almost complete crystallization of the ZrO_2 matrix and a partial reduction of the Pt moiety. The subsequent calcination step (at $T>550$°C), which has been demonstrated to be necessary to induce catalytic activity in sulfated ZrO_2 systems (26), leads to the complete reduction of Pt and, due to the presence of surface sulfates, to the aggregation of Pt into particles definitely larger than in the case of Pt supported on surface-clean (i.e., anion-free) oxides.

In contrast with what is normally observed with Pt supported on surface-clean oxides, on which the dispersion of the noble metal is good and a reduction treatment is necessary to obtain supported Pt^0 particles, on PZS systems a reductive treatment after the calcination step leads to the virtually complete deactivation of the (already scarce) Pt exposed at the surface. This is clearly shown by H_2 and CO adsorption experiments.

As the deactivation due to a reductive treatment is largely reversed by an oxidative treatment, it is thought that the species responsible for these shielding/unshielding effects are the sulfates (few, and thus not spectroscopically distinguishable) which are in contact with the exposed Pt. These sulfates would be easily reduced to sulfide and, subsequently, oxidized back to sulfates. The unusual feature of PZS catalysts is thus that, on a reduced catalyst (either *in vacuo* or in H_2), Pt would have a nonmetallic character, whereas a metallic or quasi-metallic character is acquired during a mild oxidation.

(iii) The presence of Pt induces in surface sulfates a higher thermal lability and a much easier reducibility. Also the mechanism of surface sulfate reduction is modified by the presence of Pt, as mostly H_2S (and virtually no SO_2) is produced and liberated.

Although the reduced surface sulfur can be easily reoxidized, the family of surface sulfates that has been correlated with the good catalytic performances of these systems (sulfate bands at ∼1400 and ∼1010 cm^{-1}) is eliminated first, either by vacuum thermal decomposition or by reduction, and cannot be restored by a subsequent oxidation.

ACKNOWLEDGMENTS

Thanks are due to Dr. L. Ferroni (Turin Polytechnic) for preparing the Y_2O_3-stabilized ZrO_2. Thanks are also expressed to CNR (Rome) and MURST (Rome) for financial support.

REFERENCES

1. Arata, K., *Adv. Catal.* **37**, 165 (1990).
2. Hino, M., and Arata, K., *J. Chem. Soc. Chem. Commun.* **851**, (1980).
3. Morterra, C., Cerrato, G., Pinna, F., Signoretto, M., and Strukul, G., *J. Catal.* **149**, 181 (1994).
4. Parera, J. M., *Catal. Today* **15**, 481 (1992).
5. Ebitani, K., Konishi, J., and Hattori, H., *J. Catal.* **130**, 257 (1991).
6. Ebitani, K., Konno, H., Tanaka, T., and Hattori, H., *J. Catal.* **135**, 60 (1992).
7. Davis, B. H., Keogh, R. A., and Srinivasan, R., *Catal. Today* **20**, 219 (1994).
8. Yamaguchi, T., *Appl. Catal.* **61**, 1 (1990).
9. Strukul, G., Signoretto, M., Pinna, F., Benedetti, A., Cerrato G., and Morterra, C., *in* "Advanced Catalysts and Nanostructured Materials: Modern Synthetic Methods" (W. R. Moser, Ed.), Academic Press, New York, 1996.
10. Signoretto, M., Pinna, F., Strukul, G., Cerrato, G., and Morterra, C., *Catal. Lett.* **36**, 129 (1996).
11. Sarzanini, C., Sacchero, G., Pinna, F., Signoretto, M., Cerrato, G., and Morterra, C., *J. Mater. Chem.* **5**, 353 (1995).
12. Morterra, C., Cerrato, G., Ferroni, L., and Montanaro, L., *Mater. Chem. Phys.* **37**, 243 (1993).
13. Dall' Agnol, C., Gervasini, A., Morazzoni, F., Pinna, F., Strukul, G., and Zanderighi, L., *J. Catal.* **96**, 106 (1985).
14. Boccuzzi, F., Guglieminotti, E., Pinna, F., and Signoretto, M., *J. Chem. Soc. Faraday Trans.* **91**, 3237 (1995).
15. Sayari, A., and Dicko, A., *J. Catal.* **145**, 561 (1994).
16. Ward, D. A., and Ko, E. I., *J. Catal.* **150**, 18 (1994).
17. Ward, D. A., and Ko, E. I., *J. Catal.* **157**, 321 (1995).
18. Nascimento, P., Akratopoulou, C., Oszagyan, M., Coudurier, G., Travers, C., Joly, J. F., and Védrine, J. C., *in* "Proceedings, 10th International Congress on Catalysis, Budapest, 1992" (L. Guczi, F. Solymosi, and P. Tétényi, Eds.), p. 1185. Akadémiai Kiadó, Budapest, 1993.
19. JCPDS file 4-0802.
20. Morterra, C., Cerrato, G., Pinna, F., and Signoretto, M., *J. Catal.* **157**, 109 (1995).
21. Chmelka, B. F., Went, G. T., Csencsits, R., Bell, A. T., Petersen, E. E., and Radke, C. J., *J. Catal.* **144**, 506 (1993).
22. Dicko, A., Song, X., Adnot, A., and Sayari, A., *J. Catal.* **150**, 254 (1994).
23. Bensitel, M., Saur, O., Lavalley, J. C., and Morrow, B. A., *Mater. Chem. Phys.* **19**, 147 (1988).
24. (a) Nakamoto, K., "Infrared and Raman Spectra of Inorganic and Coordination Compounds" 4th ed., Wiley, New York, 1986; (b) Little, L. H., "Infrared Spectra of Adsorbed Species" Academic Press, New York, 1966.
25. Morterra, C., Cerrato, G., Pinna, F., and Signoretto, M., *J. Phys. Chem.* **98**, 12373 (1994).
26. (a) Morterra, C., and Cerrato, G., *Pacifichem 95* (Honolulu, December 17–22, 1995), Symposium on Solid Superacids, lect. No. 25. (b) Morterra, C., Cerrato, G., and Signoretto, M., *Catal. Lett.* **41**, 101 (1996).
27. Morterra, C., Bolis, V., Cerrato, G., and Magnacca, G., *Surf. Sci.* **307–309**, 1206 (1993).
28. Detoni, S., and Hadzi, D., *Spectrochim. Acta* **11**, 601 (1957).
29. Mangnus, P. J., Riezebos, A., van Langeveld, A. D., and Moulijn, J. A., *J. Catal.* **151**, 178 (1995).
30. Kung, M. C., and Kung, H. H., *Catal. Rev. Sci. Eng.* **27**, 425 (1985).
31. Morterra, C., Cerrato, G., Emanuel, C., and Bolis, V., *in* "Proceedings, 10th International Congress on Catalysis, Budapest, 1992" (L. Guczi, F. Solymosi, and P. Tétényi, Eds.), p. 2585, Akadémiai Kiadò, Budapest, 1993.
32. (a) Eischens, R. P., Francis, S. A., and Pliskin, W. A., *J. Phys. Chem.* **60**, 194 (1956); (b) Eischens, R. P., and Pliskin, W. A., *Adv. Catal.* **10**, 1 (1958); (c) Tanaka, K., and White, J. M., *J. Catal.* **79**, 81 (1983); (d) Sheppard, N., and Nguyen, T. T., *in* "Advances in Infrared and Raman Spectroscopies," (R. J. H. Clark and R. E. Hester, Eds.), Vol. 5, p. 67. Heyden, London, 1978.
33. (a) Crossley, A., and King, D. A., *Surf. Sci.* **95**, 131 (1980); (b) Primet, M., de Menorval, L. C., Fraissard, J., and Ito, T., *J. Chem. Soc., Faraday Trans.* **81**, 2867 (1985); (c) Marchese, L., Boccuti, M. R., Coluccia, S., Lavagnino, S., Zecchina, A., Bonneviot, L., and Che, M., *in* "Structure and Reactivity of Surfaces" (C. Morterra, A. Zecchina, and G. Costa, Eds.), p. 653. Elsevier, Amsterdam, 1989.
34. (a) Jory, J. C., D'Amato, M. A., Costa, G., and Parera, J. M., *J. Catal.* **153**, 218 (1995); (b) Chao, K., Wu, H., and Leu, L., *J. Catal.* **157**, 289 (1995).
35. (a) Apesteguia, C. R., Brema, C. E., Garetto, T. F., Borgna, A., and Parera, J. M., *J. Catal.* **89**, 52 (1984); (b) Ebitani, K., Konno, H., Tanaka, T., and Hattori, H., *J. Catal.* **135**, 60 (1992).
36. Lokhov, Yu. A., and Davydov, A. A., *Kinet. Katal* **21**, 1523 (1980).
37. Tsyganenko, A. A., and Filimonov, V. N., *J. Mol. Struc.* **19**, 579 (1973).
38. Gonzales, M. R., Kobe, J. M., Fogash, K. B., and Dumesic, J. A., *J. Catal.* **160**, 290 (1996).